ANNUAL REVIEWS

Annual Review of Physical Chemistry

Dynamics at Conical Intersections

Michael S. Schuurman[1,2] and Albert Stolow[1,2,3]

[1]National Research Council of Canada, Ottawa, Ontario K1A 06A, Canada; email: michael.schuurman@nrc-cnrc.gc.ca

[2]Department of Chemistry and Biomolecular Sciences, University of Ottawa, Ottawa, Ontario K1A 0R6, Canada; email: astolow@uottawa.ca

[3]Department of Physics, University of Ottawa, Ottawa, Ontario K1A 0R6, Canada

Annu. Rev. Phys. Chem. 2018. 69:427–50

First published as a Review in Advance on February 28, 2018

The *Annual Review of Physical Chemistry* is online at physchem.annualreviews.org

https://doi.org/10.1146/annurev-physchem-052516-050721

Keywords

conical intersection, molecular dynamics, nonadiabatic, ultrafast, spectroscopy, transition state, photochemistry, photoelectron, simulation, electronic structure

Abstract

The nonadiabatic coupling of electronic and vibrational degrees of freedom is the defining feature of electronically excited states of polyatomic molecules. Once considered a theoretical curiosity, conical intersections (CIs) are now generally accepted as being the dominant source of coupled charge and vibrational energy flow in molecular excited states. Passage through CIs leads to the conversion of electronic to vibrational energy, which drives the ensuing photochemistry, isomerization being a canonical example. It has often been remarked that the CI may be thought of as a transition state in the excited state. As such, we expect that both the direction and the velocity of approach to the CI will matter. We explore this suggestion by looking for dynamical aspects of passage through CIs and for analogies with well-known concepts from ground-state reaction dynamics. Great progress has been made in the development of both experimental techniques and ab initio dynamics simulations, to a degree that direct comparisons may now be made. Here we compare time-resolved photoelectron spectroscopy results with on-the-fly ab initio multiple spawning calculations of the experimental observables, thereby validating each. We adopt a phenomenological approach and specifically concentrate on the excited-state dynamics of the C=C bond in unsaturated hydrocarbons. In particular, we make use of selective chemical substitution (such as replacing an H atom by a

methyl group) so as to alter the inertia of certain vibrations relative to others, thus systematically varying (mass-weighted) directions and velocities of approach to a CI. Chemical substituents, however, may affect both the nuclear and electronic components of the total wave function. The former, which we call an inertial effect, influences the direction and velocity of approach. The latter, which we call a potential effect, modifies the electronic structure and therefore the energetic location and topography of the potential energy surfaces involved. Using a series of examples, we discuss both types of effects. We argue that there is a need for dynamical pictures and simple models of nonadiabatic dynamics at CIs and hope that the phenomenology presented here will help inspire such developments.

1. INTRODUCTION

The excited-state dynamics of polyatomic molecules generally involve the nonadiabatic coupling of vibrational and electronic degrees of freedom, a failure of the Born–Oppenheimer approximation. Frequently, the energy associated with electronic excitations can be converted to vibrational energy on ultrafast (femtosecond) timescales, and this is often the driving force for any ensuing photochemistry (1). That conical intersections (CIs) mediate such internal conversion processes has become the de facto standard mechanism by which such ultrafast nonradiative processes are understood and their timescales justified (2). Computational simulation via ab initio calculations is now a standard tool for interpreting these phenomena (2–6). In studies of the photodissociation of polyatomic molecules, the importance of dynamics at CIs has emerged as both a guiding principle and an area of exploration (7–9).

Despite this widespread appreciation of the role of CIs in rationalizing the ultrafast timescales of these processes, there remains a lack of dynamical principles or simple models that can be applied to general molecular systems. It has long been argued that the CI is just a transition state of the excited state (4, 10, 11). By way of comparison, not only have transition-state theories been incredibly successful at the quantitative prediction of ground-state reaction rates and branching ratios, but they have also taught researchers how to think about reactive processes in terms of energy barriers and their location along a reaction coordinate, inelastic versus reactive trajectories, Polanyi rules, statistical energy redistribution and phase-space dynamics, etc. (12–16). If we take seriously the suggestion that the CI is a transition state, then we should seek analogous dynamical principles for excited-state reaction dynamics. However, rather than construct formal theories, we believe that one must begin with phenomenology as a guide. In this review, we concentrate on the dynamics of the C=C double bond, as it is the key dynamical moiety in the excited-state dynamics of the unsaturated hydrocarbons. To emphasize the notion of a local moiety in such dynamics, we introduced the term dynamophore, the part of the molecule where dynamics become localized (17), by analogy with the term chromophore, the part of the molecule where light absorption seems localized. In the examples discussed here, the CI is typically located energetically downhill from an initial Franck–Condon region, and the system therefore has considerable kinetic energy as it enters the region of strong nonadiabatic coupling. This, we argue, leads to a dynamical perspective wherein directions and velocities of approach to a CI are the crucial parameters governing outcomes. We note that this perspective is supported by a recent analytical model of nonadiabatic transition probabilities (18). The examples chosen provided us with clues as to some important aspects of vibrational motions at CIs that needed considering.

In order to systematically interrogate dynamics at CIs, we have adopted a phenomenological approach that combines ab initio spectral/dynamical simulations with the experimental method of time-resolved photoelectron spectroscopy (TRPES) (19–22). The former are computed via on-the-fly dynamics simulations that are then convoluted with quantum chemistry–based approaches to computing the time-resolved photoelectron spectrum. The latter may then be compared directly to theory and, on the basis of the degree of agreement, may guide interpretations in terms of the nonadiabatic (vibronic) evolution of the excited-state wavepacket and the roles of specific vibrational motions in these dynamics.

When interrogating the complex nonadiabatic dynamics of polyatomic molecules, we believe that systematic variation of a subset of the degrees of freedom in the problem can provide insight into the underlying mechanistic details of the nonadiabatic dynamics. In practice, the simplest method to achieve this is via selective chemical substitution (e.g., systematically replacing an H atom with a methyl group at specific locations). In particular, if we write each vibronic state in the wavepacket, $\psi_i(t, \mathbf{r}, \mathbf{R})$, as a product of an electronic component $\phi_i(\mathbf{r}; \mathbf{R})$ and a vibrational component $\chi_i(\mathbf{R})$,

$$\Psi(t, \mathbf{r}, \mathbf{R}) = \sum_i c_i(t)\psi_i(\mathbf{r}, \mathbf{R}) = \sum_i c_i(t)\phi_i(\mathbf{r}, \mathbf{R})\chi_i(\mathbf{R}), \quad 1.$$

then we can affect the states in our basis by altering either the nuclear wave function, the electronic wave function, or (as is, in practice, the general case) both. We call a chemical substitution that primarily affects the nuclear component of a state wave function an inertial effect, whereas one that significantly alters the underlying potential energy surfaces is called a potential effect. In the following, we present some background pedagogical material that we will use to interpret a series of joint theoretical/experimental studies illustrating how ultrafast processes at CIs can be probed by selective alteration of the dynamics, employing the techniques of chemical substitution. The examples we discuss in this review were chosen because they give insights into the role of vibrational motions at CIs. They encourage us to argue that there is a need for dynamical, trajectory-like pictures, perhaps analogs of those used to describe vibrational dynamics at transition states in ground-state reaction dynamics.

2. ULTRAFAST NONADIABATIC DYNAMICS VIA PUMP–PROBE SPECTROSCOPY

In our phenomenological approach, our emphasis is on understanding and interpreting femtosecond pump–probe experiments on molecular systems involving excited-state nonadiabatic processes (23). In organic photochemistry, this generally requires pump photons in the ultraviolet (UV) energy regime that, in our scenario, originate from a coherent light pulse of finite bandwidth, thus preparing a phased superposition of exact vibronic energy levels, i.e., a nonadiabatic wavepacket. Thus far, we have not discussed the determination of any particular observables, the process by which the wavepacket is projected onto a set of final states and an expectation value is computed. The determination of an appropriate experimental observable is an important point for experimentalists and theorists alike. The simulation of molecular dynamics for chemically relevant systems requires that a number of significant approximations be made. These include the level of rigor in the description of the electronic structure of the excited states, the number of nuclear degrees of freedom that are explicitly considered, and the extent to which nonadiabatic coupling is included. These approximations may be relatively trivial and easily justified and/or may be convincingly validated. However, they can just as often be motivated by computational efficacy or other concerns not related to the physics of the problem. As a result, multiple,

sometimes contradictory mechanistic narratives may be constructed for the same molecular system, depending on the approximations employed. We believe that the availability of experimentally determined observables, which may be simulated with reasonable fidelity, provides an invaluable constraint on the results of computational simulations. However, these experimentally determined constraints are of maximum utility when compared to independently computed observables using theoretical methods. We believe that one must directly compare experimental with independently calculated observables to determine a mechanism. In contrast, a given mechanistic narrative on its own may be consistent with multiple spectroscopic measurements and, hence, provides insufficient constraints.

The choice of observable employed to study these processes is a degree of freedom available to the spectroscopic investigator. The ultimate selection of an observable must be motivated by the questions that one wishes to answer. In our case, the observable should be sensitive to both the reorganization of electronic charge and the motion of the nuclei, the two classes of degrees of freedom relevant to the dynamics of nonadiabatic processes. Furthermore, the observable should be nonvanishing for the degrees of freedom being studied on the timescale of the experiment. If one were to employ electronic absorption spectroscopy to monitor the evolution of a vibronic wavepacket, possible changes in the relevant selection rules would have to be known and anticipated. For example, if the wavepacket were to undergo intersystem crossing, evolving from singlet to triplet character, the selection rules governing the allowed transitions would change drastically, leading to a drop-off in signal. In the absence of a measurable response, little could be said regarding the behavior of the wavepacket subsequent to the intersystem crossing.

We believe that the photoelectron spectrum is an observable of particular utility for studying nonadiabatic wavepacket dynamics on excited molecular electronic states. When measured on femtosecond timescales, TRPES offers insights into molecular dynamics with a level of detail that was once exclusively the domain of theoretical simulation. The energy-resolved, angle-integrated photoelectron spectrum is a particularly simple but powerful spectroscopic observable to employ in the study of excited-state wavepacket dynamics. While even more information may be obtained from energy angle–resolved spectra, we refer the reader elsewhere for a more detailed discussion (21, 22, 24–26). A schematic of the TRPES method under discussion here is presented in **Figure 1**. As shown, a hypothetical molecule is excited by a pump photon to an S_2 electronically excited state that undergoes ultrafast nonadiabatic dynamics, crossing to a lower-lying S_1 state as a function of time. In doing so, both the molecular orbital composition and the vibrational character may evolve. Probing via single-photon ionization projects this nonadiabatic wavepacket onto the molecular ionization continuum as a function of time. Because of this, changes in both electronic (Koopmans' correlations) and vibrational (Franck–Condon factors) overlaps will appear as a function of pump–probe time delay. The emitted photoelectron reflects these changes and therefore constitutes an excellent probe of the electronic and vibrational dynamics and, importantly, their couplings (22). An ultrafast pump–probe experiment conceptually involves three steps: (*a*) the pump, in which ground-state population is coherently transferred to an excited state; (*b*) the field-free evolution of the excited-state wavepacket; and (*c*) the probe, in which the excited-state wavepacket is projected onto a manifold of final states. In the simplest form, the incoherent populations in the final states are measured at the end of the two-pulse sequence, thereby creating the pump–probe signal.

If the electronic component of the wavepacket is expressed in an adiabatic electronic state basis, the electronic character of the basis may change abruptly at points localized in coordinate space, such as a CI. We note that while such a basis has well-documented formal complications arising from singular derivative couplings at points of degeneracy, it is straightforward to employ on-the-fly ab initio computations in which adiabatic electronic states may be readily computed at each and every nuclear configuration.

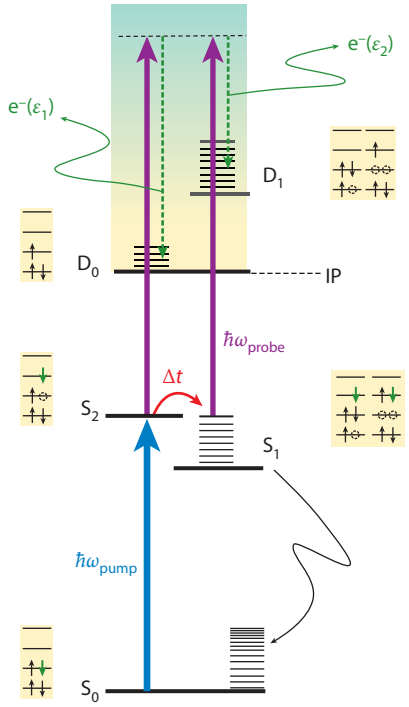

Figure 1

Schematic of a time-resolved photoelectron spectroscopy (TRPES) experiment. In this hypothetical example, the initial (time $t = 0$) wavepacket on an S_2 excited state internally converts to a lower-lying S_1 state as a function of time. The latter may undergo further crossings to the ground state. These nonadiabatic processes evolve both the electronic and vibrational character as a function of time. This wavepacket evolution is probed via projection onto a set of final (cation) states at successive time delays and varying vertical ionization potentials (IPs), and the emitted photoelectron is recorded. Due to changes in both molecular orbital composition and vibrational character, the overlap with the ionization continuum changes with time. For further details, see Reference 22.

The initial preparation of an excited state via a femtosecond-pump laser pulse creates a coherent superposition of states on the excited-state manifold—a wavepacket. Under the Born–Oppenheimer approximation, the electronic energy is presumed to display only a parametric dependence on the nuclear coordinates, so that the electronic wave functions are given by

$$\Psi(t, \mathbf{r}, \mathbf{R}) = \sum_{a=1} e^{-iE_a t/\hbar} c_a(t) \psi_a(\mathbf{r}, \mathbf{R}), \qquad 2.$$

where $c_a(t)$ are the time-dependent amplitudes, $\mathbf{r}$ and $\mathbf{R}$ are electronic and nuclear coordinates of interest in our molecular systems, and E_a is the energy of eigenstate state a. However, this basis, which formally requires the time-independent eigenstates, is not applicable in general to the excited molecular systems that are our primary interest. Instead, our theoretical apparatus involves a time-dependent nuclear basis, in which we will solve the nuclear Schrödinger equation. In particular, we will employ the ab initio multiple spawning (AIMS) approach, in conjunction with adiabatic electronic potential energy surfaces computed using multireference quantum chemical methods (27–32). We emphasize that the spawning formalism is not a semiclassical theory: It is a quantum dynamical approach that uses the classically evolving trajectories as a basis

in which to solve the nuclear Schrödinger equation. The AIMS wave function ansatz,

$$\Psi(t, \mathbf{r}, \mathbf{R}) = \sum_{I=1}^{N_s} \sum_{j=1}^{N_I(t)} C_j^I(t) \psi^I(\mathbf{r}, \mathbf{R}) \chi_j^I(\mathbf{R}; \mathbf{R}_j^I(t), \mathbf{P}_j^I(t), \gamma_j^I(t)), \quad 3.$$

employs a direct product basis of frozen Gaussian functions to describe the nuclear component. Here $\chi_j^I(\mathbf{R})$ is a Gaussian basis function on state I and $\psi^I(\mathbf{r}, \mathbf{R})$ is the corresponding electronic wave function for state I, while $\gamma_j^I(t)$ is its time-dependent phase. The time evolution of the position and momentum of the Gaussian basis functions follows classical equations of motion. The defining characteristic of the method is that the number of basis functions changes as a function of time, so that new functions are spawned where required, particularly in regions of strong coupling between the electronic states associated, for example, with curve crossings and CIs.

The advantage of this approach is that no analytic representations of the potential energy surfaces are required a priori, apart from a choice of quantum chemical theory to deploy. AIMS was the first such quantum dynamical approach to employ quantum chemical electronic structure methods to determine the requisite potential energy surfaces. Furthermore, if the dynamics are characterized by large-amplitude nuclear motion, the Cartesian coordinate basis employed in these types of computations is flexible enough to describe these displacements, and computations may be done without prior knowledge of the specific molecular distortions needed to capture the evolution of the excited-state wavepacket. Development of these so-called direct dynamics approaches remains a fruitful area of research and includes methods such as trajectory surface hopping (6, 33, 34), variational multiconfigurational Gaussian (35, 36), and multiconfigurational Ehrenfest (37), among others.

The solution of the nuclear time-dependent Schrödinger equation in this basis requires the evaluation of Hamiltonian matrix elements in a basis of classically evolving trajectories:

$$\dot{\mathbf{C}}(t) = -i\mathbf{S}^{-1}(\mathbf{H} - i\dot{\mathbf{S}})\mathbf{C}(t). \quad 4.$$

Here $\mathbf{S}$ is the overlap matrix of the classically evolving Gaussian basis functions, $\mathbf{C}(t)$ are the complex amplitudes, and $\mathbf{H}$ is the Hamiltonian matrix evaluated in the trajectory basis:

$$\begin{aligned} H_{Ij I'j'} &= \langle \phi^I(\mathbf{r}; \mathbf{R}) \chi_j^I(\mathbf{R}) \,|\, H_e(\mathbf{r}, \mathbf{R}) + T_{\mathbf{R}} \,|\, \phi^{I'}(\mathbf{r}; \mathbf{R}) \chi_{j'}^{I'}(\mathbf{R}) \rangle \\ &= \langle \chi_j^I(\mathbf{R}) \,|\, H_{II'}(\mathbf{r}; \mathbf{R}) \,|\, \chi_{j'}^{I'}(\mathbf{R}) \rangle + \langle \chi_j^I(\mathbf{R}) \,|\, T_{\mathbf{R}} \,|\, \chi_{j'}^{I'}(\mathbf{R}) \rangle \delta_{II'}, \end{aligned} \quad 5.$$

where H_e and $T_{\mathbf{R}}$ are the electronic Hamiltonian and nuclear kinetic energy ($-\sum_{i=1}^{N^a} \nabla_i^2 / 2M_i$), respectively. Following integration over electronic coordinates, one obtains an analytically integrable nuclear kinetic energy integral over nuclear basis functions, as well as terms arising from the electronic Hamiltonian:

$$\langle \chi_j^I(\mathbf{R}) \,|\, H_{II'}(\mathbf{r}; \mathbf{R}) \,|\, \chi_{j'}^{I'}(\mathbf{R}) \rangle = \langle \chi_j^I(\mathbf{R}) \,|\, E_e^I(\mathbf{R}) \delta_{II'} - 2D_{II'} - G_{II'} \,|\, \chi_{j'}^{I'}(\mathbf{R}) \rangle, \quad 6.$$

where $E_e^I(\mathbf{R})$ is the energy of adiabatic state I and

$$D_{II'} = \sum_{i=1}^{N^a} \frac{1}{2M_i} \langle \phi^I(\mathbf{r}; \mathbf{R}) \,|\, \nabla_i \phi^{I'}(\mathbf{r}; \mathbf{R}) \rangle \cdot \nabla_i, \quad 7.$$

$$G_{II'} = \sum_{i=1}^{N^a} \frac{1}{2M_i} \langle \phi^I(\mathbf{r}; \mathbf{R}) \,|\, \nabla_i^2 \phi^{I'}(\mathbf{r}; \mathbf{R}) \rangle. \quad 8.$$

The $D_{II'}$ and $G_{II'}$ are the derivative and scalar couplings between states I and I'. For the results shown here, which are obtained via ab initio propagation, the $G_{II'}$ are excluded for computational tractability. The $D_{II'}$ terms may be efficiently evaluated using quantum chemical methods via the

expression

$$\mathbf{f}_{II'} = \langle \phi^I(\mathbf{r};\mathbf{R}) \,|\, \nabla \phi^{I'}(\mathbf{r};\mathbf{R}) \rangle = \frac{\langle \phi^I(\mathbf{r};\mathbf{R}) \,|\, \nabla H_e \,|\, \phi^{I'}(\mathbf{r};\mathbf{R}) \rangle}{E_{I'} - E_I}. \quad 9.$$

As implied by the energy difference denominator, this term becomes particularly large as the energy difference between states I and I' becomes small, and it is singular when the two electronic states are degenerate. If the degeneracy at the point of crossing is lifted linearly, then the crossing between states I and I' is termed a CI. As the energy difference between the electronic states decreases, the term coupling the basis functions on different states in Equation 5 gets similarly large, and wavepacket amplitude may be rapidly transferred between states. As implied by Equation 7, the magnitude of the matrix element is large when the nuclear velocity is large and parallel to the direction implied by the interstate coupling. Thus, in the limit of low (or high) velocity, one expects adiabatic (or diabatic) behavior.

3. CONICAL INTERSECTIONS: TRANSITION STATES OF THE EXCITED STATE

Considerable theoretical effort has been expended investigating the role of various intersection topographies in the excited-state dynamics (38–42). The phenomenology of CIs has led us to appreciate that specific topographies lead to specific reactive outcomes for trajectories passing through the region of strong nonadiabatic coupling. We currently lack, however, a deeper understanding of what governs these processes: We do not have any simple rules, analogs of transition-state theory, to guide our thinking. A major aim of our joint experimental-theoretical research program is to discover such rules, assuming they exist.

Using a perturbation theory treatment (2), the coordinate space in which the degeneracy is lifted linearly at a point of intersection between two nonrelativistic electronic states can be shown to be two-dimensional and is termed the branching space. The directions that define these internal coordinates (in terms of nuclear displacements) can be readily determined from the electronic structure of the intersecting surfaces. The so-called **g** and **h** directions, respectively the energy difference gradient and nonadiabatic coupling vectors, are given by

$$\mathbf{g} = \frac{1}{2}\left(\langle \Psi^I(\mathbf{r};\mathbf{R}) \,|\, \nabla H_e(\mathbf{r};\mathbf{R}) \,|\, \Psi^I(\mathbf{r};\mathbf{R}) \rangle - \langle \Psi^J(\mathbf{r};\mathbf{R}) \,|\, \nabla H_e(\mathbf{r};\mathbf{R}) \,|\, \Psi^J(\mathbf{r};\mathbf{R}) \rangle \right), \quad 10.$$

$$\mathbf{h} = \langle \Psi^I(\mathbf{r};\mathbf{R}) \,|\, \nabla H_e(\mathbf{r};\mathbf{R}) \,|\, \Psi^J(\mathbf{r};\mathbf{R}) \rangle, \quad 11.$$

and correspond to nuclear displacements that take a trajectory through the CI region. Necessarily, the remaining $N-2$ internal degrees of freedom orthogonal to this space preserve the degeneracy and are termed the seam space. If **g** and **h** are rotated so as to be orthogonal to each other (now denoted by **x** and **y**), these directions, plus $N-2$ mutually orthogonal seam-space directions, form a set of intersection-adapted coordinates (38). In this way, the internal degrees of freedom may be differentiated into those that result in passage through a region of CI and those that move along a region of intersection. If a CI may be thought of as a point at which the adiabatic electronic character changes suddenly, then the former coordinates are those that enable passage through a region of strong coupling and can be thought of as the reaction coordinates for excited-state dynamics. Further, it also follows that how a trajectory approaches a CI along one of these reactive coordinates (i.e., from which direction and with what velocity) can be a determining factor in the outcome of a nonadiabatic transition process. The manner of approach to the CI has has been described as a mechanism to route trajectories to particular electronic/product states (39, 43). From our point of view, the use of chemical substitution as a method for systematically varying

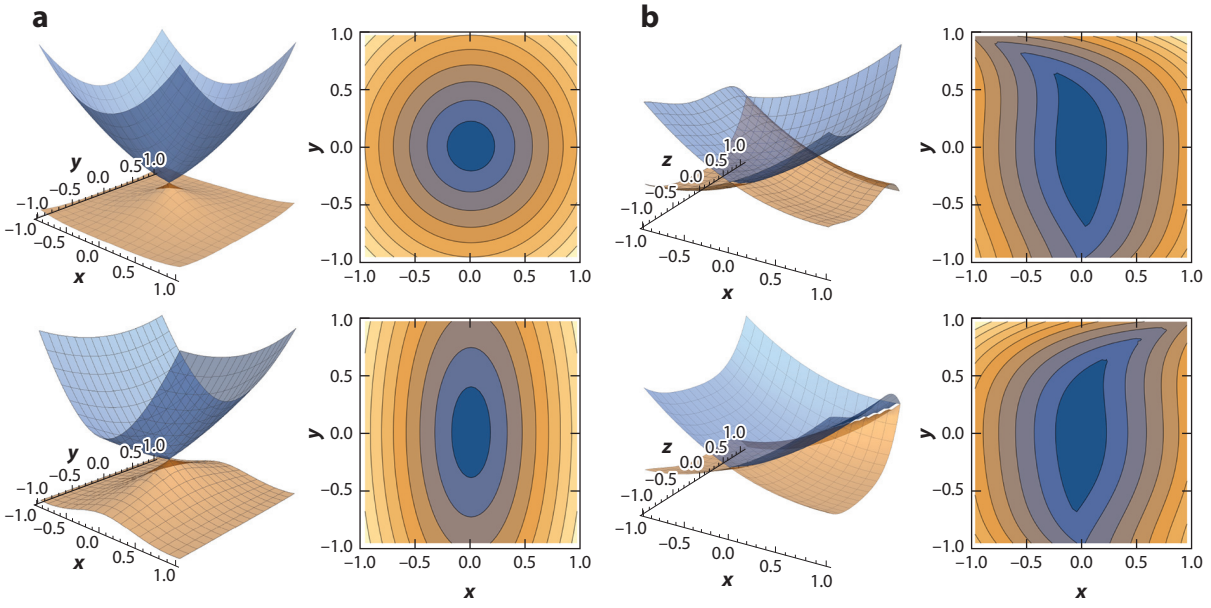

Figure 2

Schematic of (*a*) the two-dimensional branching space and (*b*) the intersection seam of a hypothetical CI in effective mass-weighted coordinates x and y. (*a*, *Top*) $\omega_x/\omega_y = 1$. (*a*, *Bottom*) $\omega_x/\omega_y = 0.2$. Analogous to the well-known skew angles in A + BC reactive potential energy surfaces, panel *a* illustrates how inertial effects can change the skew/asymmetry of a CI, potentially leading to changes in diabatic versus adiabatic passage. This point is also discussed in Reference 18. Panel *b* evinces how intersection seams may be altered via changes to the underlying potentials. We argue here that such inertial and potential effects may be achieved via selective chemical substitution.

the direction and velocity of approach to a CI, as illustrated in **Figure 2**, allows us to probe the role of vibrational dynamics at CIs.

3.1. Vibrational Degrees of Freedom at Conical Intersections

Models for nonadiabatic transitions in molecules have long recognized that the specific vibrational degrees of freedom that mediate radiationless transitions between electronic states are often a very small subset of the entire internal coordinate space. The **g** and **h** directions discussed above that span the branching space can be expressed in terms of normal modes, allowing passage through the intersection region to be interpreted using a vibrational basis. Constructing models that allow for the a priori prediction of the relevant motions is a major goal in this area of research.

Early models, based on so-called energy gap laws (44–46), described radiationless transfer processes using perturbative (weak coupling) golden rule rate laws. This approach identified those modes that carry the majority of the amplitude of the nonadiabatic coupling matrix element (promoting modes) and those highly anharmonic accepting modes that engender Franck–Condon overlap of the vibrational wave functions between two coupled electronic states.

An early application of excited-state ab initio quantum chemistry to dynamics, these models were used to rationalize the observation, or lack thereof, of fluorescence in organic chromophores. However, the identification of those matrix elements that carried the preponderance of the magnitude could only hint at the mechanistic/photochemical processes underlying the ultrafast decay.

The presumption of weak coupling in the vibrational manifold of states is not consistent with the ultrafast decay processes seen in the excited-state dynamics of many systems. A powerful approach for describing the time evolution of the vibronic wavepacket was developed in which the coupled electronic states are expanded about a point in coordinate space and parameterized so that the vibrationally mediated couplings due to particular normal modes are explicitly considered. The vibronic Hamiltonian methods developed by Köppel, Domcke & Cederbaum (47, 48) have been widely employed to propagate vibronic wavepackets and simulate various spectroscopic observables, including absorption and photoionization spectra (23). In this approach, a basis of quasi-diabatic states are expanded about a particular geometry using a polynomial expansion in terms of dimensionless normal coordinates, Q:

$$H = H_0\mathbf{I} + \mathbf{V} = \frac{1}{2}\sum_i \omega_i \left(-\frac{\partial^2}{\partial Q_i^2} + Q_i^2\right)\mathbf{I} + \begin{pmatrix} \sum_i \kappa_i^1 Q_i + \ldots & \\ \sum_i \lambda_i Q_i + \ldots & \sum_i \kappa_i^2 Q_i + \ldots \end{pmatrix}. \quad 12.$$

The various coupling parameters κ, λ may be readily determined via ab initio computation, with the truncation order (i.e., linear, quadratic, etc.) of expansion denoting the model. These models are often used to simulate spectroscopic observables characterized by ultrafast population transfer between electronic states. In general, to achieve quantitative accuracy, only a subset of vibrational modes need be considered: specifically, those that modulate the energy difference between the two states and those that modulate the interstate coupling. The former are termed tuning modes and are described by the diagonal κ coefficients in Equation 12, whereas the latter are termed coupling modes and are parameterized by the λ terms. While higher-order terms can lead to quantitative descriptions of anharmonic effects in spectroscopic applications (49–52), the polynomial nature of the expansion of the diabatic potential surfaces makes a general description of dynamics involving large-amplitude vibrational motions, such as isomerization or dissociation, very challenging.

Chemical processes, by definition, involve bond breaking and formation, necessarily requiring large-amplitude nuclear motion. Since the AIMS simulation approach described above involves on-the-fly determination of the potential energy surface, no analytic representation of the underlying potential surfaces is required. The preeminent advantage of this approach is that if the dynamics involve highly anharmonic motion, including isomerization and/or bond cleavage, such a trajectory basis method will be able to identify and predict which motions will be important for describing the photochemical dynamics of interest. Recall that one important difference between ground-state dynamics at transition states and excited-state dynamics at CIs is that the former are usually energetically uphill, whereas the latter are frequently downhill. The trajectory-based picture we have in mind, therefore, is one where steep potential gradients fire trajectories through CIs, and it is the direction and speed of approach, rather than the dwell time, that matter most. Intuitively, since the time of passage through the CI region is so short, it is not possible for all internal degrees of freedom to participate significantly in the dynamics (53, 54). Some will be too slow and will essentially be frozen spectators during the ultrafast nonadiabatic passage. Therefore, one should not in principle expect that all degrees of freedom will be relevant to the dynamics. Furthermore, since the energy distribution is far from equilibrium and there is insufficient time for randomization, it would be difficult or inadvisable to attempt to construct microcanonical models of these dynamical processes. This again points to the need for a dynamical rather than a statistical perspective.

3.2. Gradient-Directed Dynamics: The C=C Bond

We focus here on excited-state dynamics in unsaturated hydrocarbons that involve strongly gradient-directed processes on excited electronic states. The chromophore from which the

lowest-energy, optically bright transition originates in many organic and biological molecules corresponds to an electronic transition on the unsaturated hydrocarbon moiety, the C=C bond(s). For example, an electronic excitation from an occupied π orbital to an antibonding π^* orbital is a common type of transition for these processes and generally occurs at UV frequencies. Unsaturated hydrocarbons exhibit a number of these $\pi\pi^*$ transitions in the 5–8 eV range and are the focus of the present discussion.

The simplest unsaturated hydrocarbon is ethylene, C_2H_4. This molecule has been studied extensively for decades and has been the subject of numerous benchmark dynamical and spectral simulations (55–60). The lowest-lying electronic transition begins at about 6.5 eV and corresponds to excitation from a π orbital to a 3s Rydberg orbital. However, there is strong nonadiabatic coupling between the π3s and $\pi\pi^*$ states, leading to a very short lifetime of the vibronic levels in the 3s manifold and a concomitantly broadened absorption band. The dynamics of most interest involve the $\pi\pi^*$ state. Ab initio computation has long shown that the resultant molecular motions involve torsion about the C=C bond (thereby minimizing the antibonding interactions of the π^* orbital), followed by pyramidalization at one of the C centers. Additionally, if this large-amplitude motion is accompanied by a rocking of the CH_2 group, dynamics studies have predicted (consistent with experimental observations) (57) conical intersection pathways involving three-center C–C–H bonds or even excited-state H-shifts to form ethylidene-like structures (58, 61–64).

Twisted pyramidalization motions were recognized as general features of dynamics in unsaturated hydrocarbons. Theoretical investigations into the origin of the pyramidalization quickly identified the sudden polarization across the double bond that resulted from the out-of-plane distortions of a terminal methylene group (65, 66). Vibrations along this internal coordinate bring about the formation of a partial negative charge on the pyramidalizing carbon, resulting in an abrupt increase in the permanent dipole of the molecule. In the case of ethylene, such structures are associated with minimum-energy CIs: population funnels that result in rapid electronic deexcitation. Recent TRPES experiments (59, 60) are in broad agreement with myriad ab initio simulation results in determining an excited-state lifetime of $<$100 fs for the initially prepared $\pi\pi^*$ state.

This timescale is representative of the examples that follow. For the internal conversion processes to occur so rapidly, often on timescales equivalent to only a few vibrational periods along key modes, the relevant potential surfaces generally exhibit steep gradients from the initial Franck–Condon region (in which the initial wavepacket may be localized following femtosecond pump preparation) to the region of strong nonadiabatic coupling and the energetically accessible CIs. The primary consequence of these surface topographies is that there is insufficient time during the rapid passage through the region of strong coupling for vibrational energy to redistribute widely among the various internal degrees of freedom (53, 54). This likely precludes the possibility of a (microcanonical) phase-space treatment of dynamics at CIs for isolated systems. Rather, the relevant phase-space picture of the wavepacket is one in which fairly localized trajectories follow gradients of steepest descent to a region of CI, at which point specific vibrational motions govern the population transfer between coupled electronic states.

4. SUBSTITUENT EFFECTS ON DYNAMICS AT CONICAL INTERSECTIONS

The coupling of electronic states via CIs is mediated by the vibrational degrees of freedom. As discussed above, the vibrational modes that lead to appreciable modulation of the energy gap between the involved electronic states and their interstate nonadiabatic coupling often form a small subset of the total vibrational space. These vibrational coordinates may often be identified

via a combination of ab initio computation and chemical intuition. In terms of a trajectory-based narrative, this means that the direction of approach to the CI matters. As a nonlocal derivative coupling, passage through CIs is also governed by the velocity at which the CI is approached: Very low (or high) velocity is expected to lead to adiabatic (or diabatic) passage. These general aspects of dynamics at CIs lead us to consider a phenomenological approach based on the techniques of chemical substitution. In particular, we discuss here two specific chemical substitution strategies for probing ultrafast nonadiabatic processes: (*a*) selectively altering the nuclear momenta as they pass through a region of strong coupling, and (*b*) selectively altering the energetic location of curve crossings, and thus the potential barriers or gradient-directed motions in the vicinity of a CI. As discussed above, we refer to the former as inertial effects and the latter as potential effects. What follows is an overview of several joint theoretical-experimental studies illustrating how systematic chemical substitution can influence dynamics at CIs in a readily rationalizable manner. Using these examples, we argue that the interplay between inertial and potential effects is the key to using chemical substitution as a tool for illuminating vibrational dynamical at CIs.

4.1. Inertial Effects

An inertial substituent is assumed to be an electronically inert chemical moiety that serves to simply slow down or speed up certain vibrational motions by increasing or decreasing the effective mass along a particular vibrational coordinate. Isotopic substitution would be the ideal example of this approach, but here the maximum predicted effect (via deuteration) is often too small to be very useful using current experimental techniques. Therefore, we have routinely used a methyl group as a surrogate, mass-15 "H atom" to produce a much more pronounced inertial effect, particularly when large-amplitude H-atom motion is important in the nonadiabatic dynamics. Importantly, the ability of synthetic organic chemistry to selectively methylate chosen locations within a molecule offers us the opportunity to add inertia to selected internal motions. This, in turn, allows us to probe the dynamical consequences of reducing the velocity of certain vibrational motions relative to others. We note, however, that the assumption that such substitutions have little potential effect is not always warranted. As an example of a potential effect, the nonadiabatic transitions between electronic states of valence and Rydberg character may be significantly altered by methyl substitution because of the differential stabilization of the Rydberg states relative to the valence states (67). Nevertheless, in the examples that follow, we demonstrate that the methyl substitution technique can result in significantly different excited-state dynamics (including excited-state lifetimes and decay channels predicted via simulation) even when there are subtle potential effects.

4.1.1. Acrolein: velocity matters. By systematically moving a methyl substituent to different locations on the same molecular frame, one can alter the relative inertia of certain vibrations with respect to others, while keeping the overall density of states roughly constant. An example is the Norrish type 1 photoreaction of the unsaturated aldehydes and ketones, the simplest of which is the α, β-enone acrolein (propenal) (68). The excited-state photoinitiated dynamics of acrolein are depicted in **Figure 3**. The UV (200 nm)–absorbing state is the $S_2(\pi\pi^*)$ state, analogous to that in ethylene. The bright S_2 state has a CI with the lower-lying but dark $S_1(n\pi^*)$ state. The excited-state lifetime of the S_2 state is extremely short and, as in ethylene, is determined by passage through the S_2–S_1 CI via large-amplitude torsion of the terminal methylene group. Motion on the steep $S_1(n\pi^*)$ potential leads to a second CI, in this case between the S_1 state and the S_0 ground state, as depicted in **Figure 3**. Diabatic versus adiabatic passage though this second CI governs the fate of the excited molecule. Diabatic passage preserves the $S_1(n\pi^*)$ electronic character, leading to triplet formation and subsequent α-cleavage photochemistry (i.e., HCO and C_2H_3 radical

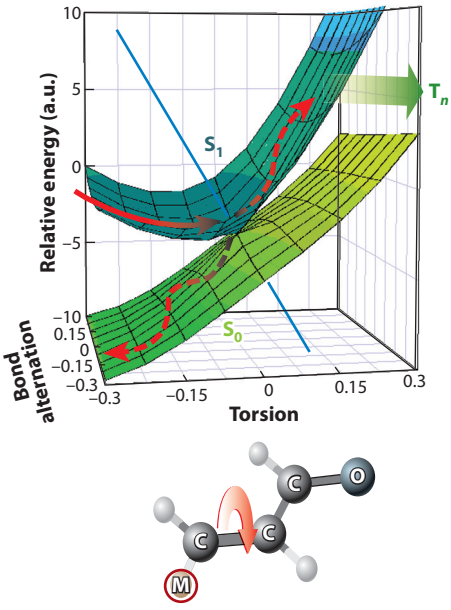

Figure 3

Excited-state $S_1(n\pi^*)$ potential energy surface of acrolein and its intersection with the S_0 ground state, as a function of the C=C torsional angle. Systematic methyl substitution significantly affects both the S_1 lifetime and the triplet (T_n) state product (i.e., α-cleavage) yields. In particular, when the methyl group, labeled M, is placed on the terminal methylene, the triplet yield essentially vanishes and the S_1 state lifetime significantly decreases. Only in this position does the methyl slow down the C=C torsional motion, leading to a more adiabatic passage through the S_1–S_0 CI to the ground state, avoiding vibrational redistribution on the S_1 potential and the triplet manifold. At all other locations of M, C=C torsion remains fast, leading to a more diabatic passage that retains S_1 character, ultimately forming triplet-state products.

products), typical of aldehydes and ketones. In contrast, adiabatic passage leads to formation of the hot ground-state molecule, subsequent singlet-state photochemistry, and molecular products (e.g., CO, C_2H_4, H_2).

We have found that the location of a single methyl substituent greatly affects the excited-state lifetime and singlet-triplet branching (68). Locating the methyl group on the central carbon atom (i.e., methacrolein) or carbonyl group carbon atom (i.e., methyl vinyl ketone) has only a small effect. Surprisingly, locating the methyl group on the terminal methylene (i.e., crotonaldehyde) simultaneously reduces the excited-state lifetime and, remarkably, completely turns off the triplet photochemistry channel. These results cannot be easily rationalized in terms of energetic shifts caused by methylation (which are small), changes in the CI topography (all three topographies are similar), or changes in the density of states (all three densities are similar): In other words, it appears that methyl substitution in the α,β-enones has an inertial rather than a potential effect. A simple model consistent with this result is depicted in **Figure 3**. The CI between S_1 and S_0 is achieved via large-amplitude torsional motions of the terminal methylene group, originating at the S_2–S_1 CI. When this terminal methylene group contains only H atoms (acrolein), the torsional velocity is high. This rapid motion leads to a more diabatic passage through the S_1–S_0 CI. Remaining on the $S_1(n\pi^*)$ potential, spin-orbit coupling leads to triplet state formation and subsequent α-cleavage photochemistry. In contrast, replacing a methylenic H atom with a methyl group adds significant inertia (mass 15 versus mass 1) to this torsional motion. This slows down

the torsional velocity and leads to a more adiabatic passage through the S_1–S_0 CI and, hence, a facile return to the S_0 ground state. This reduces the excited-state lifetime, simultaneously turning off the triplet photochemistry channel.

These types of studies give some first hints of the important role of inertia on vibrational dynamics at CIs. From a chemical control point of view, it is remarkable that the specific location of a methyl group has such a dramatic effect on the excited-state dynamics and photochemical branching ratios, a consequence not predictable from a structure–function perspective alone.

4.1.2. Allene: twisted sisters. We studied the ultrafast excited-state dynamics of allene (propadiene) and a series of its increasingly methylated analogs [1,2-butadiene (1,2-BD); 1,1-dimethylallene (DMA); and tetramethylallene (TMA)] to elucidate the effects of the methylation on branching between different CIs (69). In the allene ground state, the π orbitals on the terminal carbons are orthogonal. In contrast, the $\pi\pi^*$ excited state is expected to be twisted, and this should therefore bring the terminal π orbitals into overlap, improving stabilization. Using TRPES, 1,2-BD, DMA, and TMA were pumped at 200 nm to their bright $S_1(\pi\pi^*)$ state and probed at 267 nm. Using AIMS at the MR-FOCI(4,4) level of theory, we simulated the excited-state dynamics in these molecules, calculating dynamical pathways and excited-state lifetimes. Using the AIMS trajectories, we also directly simulated the TRPES spectra (70), which are in good agreement with experiment.

In all molecules, we found two distinct CI pathways characterized by twisting about the central allenic CCC axis followed by (*a*) pyramidalization at one of the terminal carbon atoms or (*b*) bending of the allene C–C–C moiety. The twisting ψ and bending χ coordinates are defined and shown in **Figure 4*e***. The first set of CIs we call Tw-Py geometries, corresponding to rotation (twisting) about the dihedral angle ψ followed by pyramidalization of the terminal CH_2 units. This Tw-Py behavior is essentially that of a substituted ethylene. The second set of CIs we call Tw-B geometries, corresponding to rotation (twisting) about the dihedral angle ψ followed by bending of the CCC backbone, defined by coordinate χ. These two CI types are illustrated in **Figure 4*e***. All four molecules show a fast 30–50-fs decay of the initially excited $\pi\pi^*$ state from the Franck–Condon region. The subsequent steps depend on the degree of methylation, with TMA's excited-state lifetime being an order of magnitude longer than that of 1,2-BD. Although the pathways from the Franck–Condon point to both CIs are essentially barrierless in all molecules, the Tw-Py CIs are favored (60:40) in most cases, an observation partly attributable to twisting usually being faster than bending in these excited states. Importantly, the two degrees of freedom ψ and χ are strongly coupled and, once the local minimum at $\psi = 0$ has been reached, there exists a significant barrier to bending along χ. **Figure 4*a–d*** evinces this by plotting the ab initio computed two-dimensional S_1 potential energy surfaces as a function of the reduced-mass-weighted ψ and χ coordinates for allene, 1,2-BD, DMA, and TMA. It can be seen that twisting modulates and reduces the propensity for bending. This can be readily understood from a chemically intuitive picture wherein large-amplitude twisting in the excited state improves π overlap and leads to increased stabilization/delocalization of the π orbital system, thereby stiffening the CCC unit (i.e., reducing the bending amplitude). We further note that ultrafast internal conversion to the ground state is preferentially mediated by the Tw-Py CI, whereas trajectories that maintain quasi-planarity (i.e., the Tw-B CI) remain trapped in S_1 for more extended periods. In TMA, full methylation at both terminal carbons significantly increases the reduced mass for twisting motions. Consequently, the bending of the allenic CCC unit is relatively uninhibited at early times. Large-amplitude bending avoids the Tw-Py CI, thereby trapping the wavepacket in the excited state for longer times. Interestingly, even though both types of CI are energetically downhill and configurationally accessible, it is the relative timescales of two large-amplitude motions,

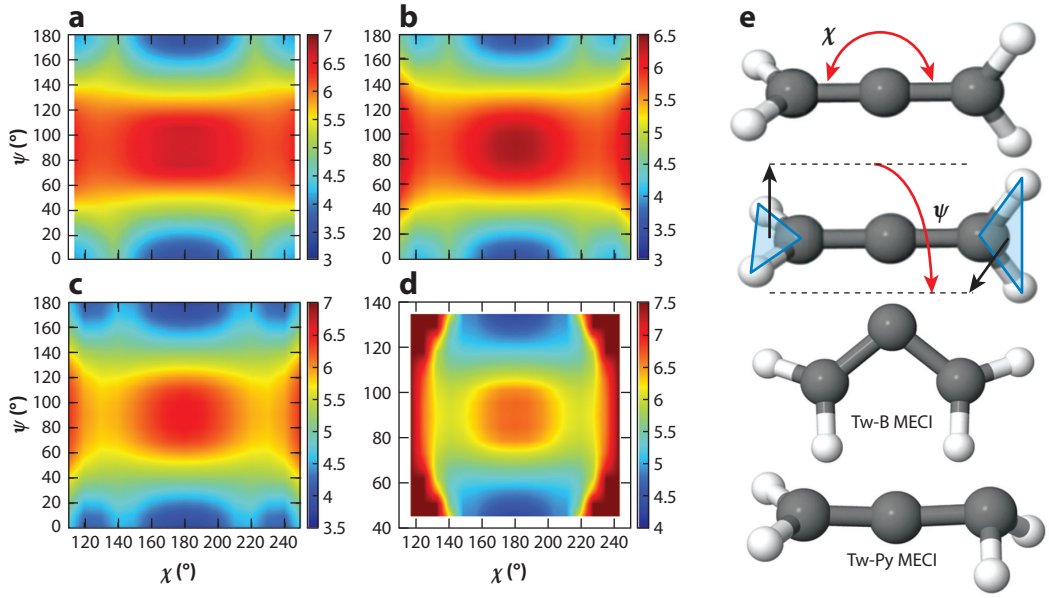

Figure 4

We show two-dimensional potential energy surfaces for (*a*) allene, (*b*) 1,2-butadiene, (*c*) 1,1-dimethylallene, and (*d*) TMA in the space spanned by the twisting ψ and C–C–C bending χ reduced-mass-weighted coordinates defined by the molecular internal coordinates shown in panel *e* (*top*). Increasing methylation (i.e., going from panel *a* to panel *d*) changes the relative curvature of the (reduced-mass-weighted) potentials in the Franck–Condon region. This in turn significantly affects the short-time dynamics. Whether twisting is fast (allene) or slow (TMA) compared to bending determines which of the S_1–S_0 CI seams is accessed first, Tw-Py or Tw-B, as shown in panel *e* (*bottom*). Abbreviations: MECI, minimum-energy conical intersection; TMA, tetramethylallene; Tw-B, twisting followed by bending; Tw-Py, twisting followed by pyramidalization.

bending versus twisting, that determine the dynamical outcome. This again illustrates the need for dynamical (i.e., trajectory or wavepacket) models of nonadiabatic processes in excited states.

4.2. Potential Effects

While all chemical substitutions alter the underlying potential energy surfaces in some fashion, selectively altering particular regions of the potential energy surface, while leaving the dominant chromophore (i.e., the spectroscopy) relatively unperturbed, can have a profound effect on the nonadiabatic dynamics. These potential effects can be thought of as affecting branching between different relaxation pathways by tilting the relevant potential energy surfaces one way or the other, or by shifting the relative energies of the coupled electronic states so that their crossing point (which is outside the Franck–Condon region) is displaced. In the first example below (Section 4.2.1), successive methylation is employed to systematically (*a*) increase and (*b*) displace along an internal coordinate the energetic barrier to a CI between the valence $\pi\pi^*$ and Rydberg π3s states in methylated ethylenes. The effect on the excited-state lifetime from ethylene to tetramethylethylene is profound, increasing it by more than two orders of magnitude. Alternatively, in a molecule where there exist multiple CI-mediated decay pathways, chemical substituents can be employed to increase the potential barrier along one decay pathway and/or to decrease the barrier along another, thereby significantly altering the branching ratio between different CIs. The second example below (Section 4.2.2) details a study in which a cyano group substituent

is employed to direct large-amplitude motion toward a particular CI decay pathway, a potential effect that relates to the electron-donating (or electron-withdrawing) nature of the substituent.

4.2.1. Methyl-substituted ethylenes: from early to late. We studied the excited-state dynamics of the methylated ethylenes *cis*-butene, *trans*-butene, trimethylethylene, and tetramethylethylene, following initial excitation to their respective π3s Rydberg states (67). The corresponding laser wavelengths used were: 200-nm pump and 225-nm probe (*cis*-butene and *trans*-butene); 216-nm pump and 267-nm probe (trimethylethylene); and 216–232-nm pump and 267-nm probe (tetramethylethylene). As illustrated in **Figure 5**, the initally excited π3s Rydberg state crosses over to the ππ* valence state on ultrafast timescales. The latter subsequently decays to the S_0

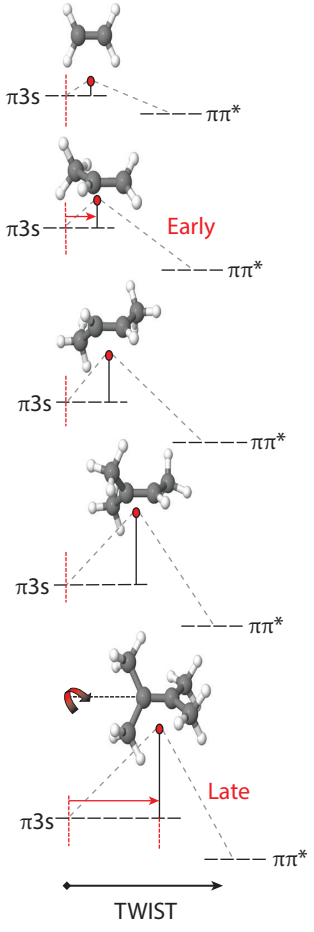

Figure 5

Schematic of the initial π3s Rydberg (reactant) and final ππ* valence (product) states along the torsion internal coordinate, ranging from ethylene (*top*), which has no methyl substituents, to tetramethylethylene (*bottom*), which is fully methylated. Increasing methylation lowers the energy of the π3s state relative to the ππ* state, displacing their curve crossing the CI later along the torsional coordinate while simultaneously increasing the barrier to accessing the CI. In each case, the relative energetic location of the CI is given by a red dot, with the corresponding CI geometry shown directly above it. This transition from early (reactant-like) to late (product-like) is reminiscent of the Polanyi rules for ground-state reaction dynamics.

ground state. We found that the decay rate varies greatly with substituent: The dimethylethylenes (*cis*-butene and *trans*-butene) and trimethylethylene show an ultrafast decay (~20 fs), whereas the fully methylated tetramethylethylene shows a decay rate 2–4 orders of magnitude slower, depending on the pump laser wavelength.

The calculated minimum-energy CIs connecting the $\pi 3s$ Rydberg state to the $\pi\pi^*$ valence state are of a twisted geometry, with a torsional angle that increases with the degree of methylation. Furthermore, the energy gap between the initial Franck–Condon region on the $\pi 3s$ state and the CI also increases with methylation. This is because methylation energetically lowers the $\pi 3s$ Rydberg state relative to the $\pi\pi^*$ valence state. The crossing point between the Rydberg and valence states therefore appears, upon increasing methylation, later along the reaction coordinate, i.e., at increasing torsional angles. Furthermore, due to the stabilization of the Rydberg state relative to the valence state, there also now appears an energetic barrier between the $\pi 3s$ minimum and the CI, which grows with increased methylation. As discussed above, we seek relations between transition-state theory, ground-state reaction dynamics, and the idea of a generalized reaction coordinate for dynamics at CIs. For all the methylethylenes, the CI's **g** vector is primarily torsion. The **h** vector, in contrast, varies considerably upon methylation, from more ethylene-like (C–H stretch) in the dimethylethylenes to more pyramidalization-like in tetramethylethylene, as depicted by the ball-and-stick models in **Figure 5**.

Importantly, upon methylation and relative to the initial Franck–Condon point, the CI occurs at relatively higher energy and correspondingly at geometries further displaced (i.e., later) along the torsional coordinate. We consider torsion in methylethylenes as a quasi-one-dimensional reaction coordinate and the CI as the transition state between the (planar) $\pi 3s$ reactant and the (90° twisted) $\pi\pi^*$ product. In the dimethylethylenes, the transition state is early along the reaction coordinate (at about 47°), has a small barrier, and is more reactant-like ($\pi 3s$) in nature. In tetramethylethylene, the transition state is late (at about 63°), has a large barrier, and is more product-like ($\pi\pi^*$) in nature. Trimethylethylene, with a transition state located at about 57° of torsion, is intermediate between the previous two cases and has a geometry that contains aspects of both. In tetramethylethylene, the late transition state and concomitant high barrier mean that accessing the CI region is much more difficult in this molecule. In addition, the pyramidalization-like **h** vector of the CI in tetramethylethylene may be subject to steric effects from the methyl groups, further thwarting access to the CI region. The combination of these two effects leads to the observed much longer excited-state lifetimes in tetramethylethylene. These examples lead us suggest the application of concepts from ground-state reaction dynamics, such as the Polanyi-rule notions of early and late transition states, to dynamics at CIs.

4.2.2. Methyl-substituted acrylonitriles: Proximity matters. Heteroatoms will undoubtedly have effects on the electronic structure of potential energy surfaces and constitute another broad avenue of exploration in the effects of chemical substituents on dynamics at CIs. Acrylonitrile (AN), or cyano-substituted ethylene, as well as its methylated analogs, was recently studied by TRPES and ab initio simulation (71). Here, the inertial methyl substituents were placed at the 2- and 3-carbon atoms (C2 and C3, respectively), and their corresponding TRPES spectra and AIMS dynamical simulations were compared to those of AN. The 200-nm pump employed in all cases prepared a $\pi\pi^*$ state primarily localized on the ethylenic carbons. The large-amplitude motions that followed excitation, as determined from simulation, involved the well-known twist about the ethylenic C=C bond, followed by pyramidalization. However, unlike in ethylene, the two carbon atoms here are chemically inequivalent, with a methyl substituent at C2 in the case of *cis*-2-methacrylonitrile (MeAN) and at C3 in the case of *cis*-3-methacrylonitrile or *cis*-crotonitrile (CrN) (see **Figure 6**). Were inertial effects dominant, we would expect that the excited-state

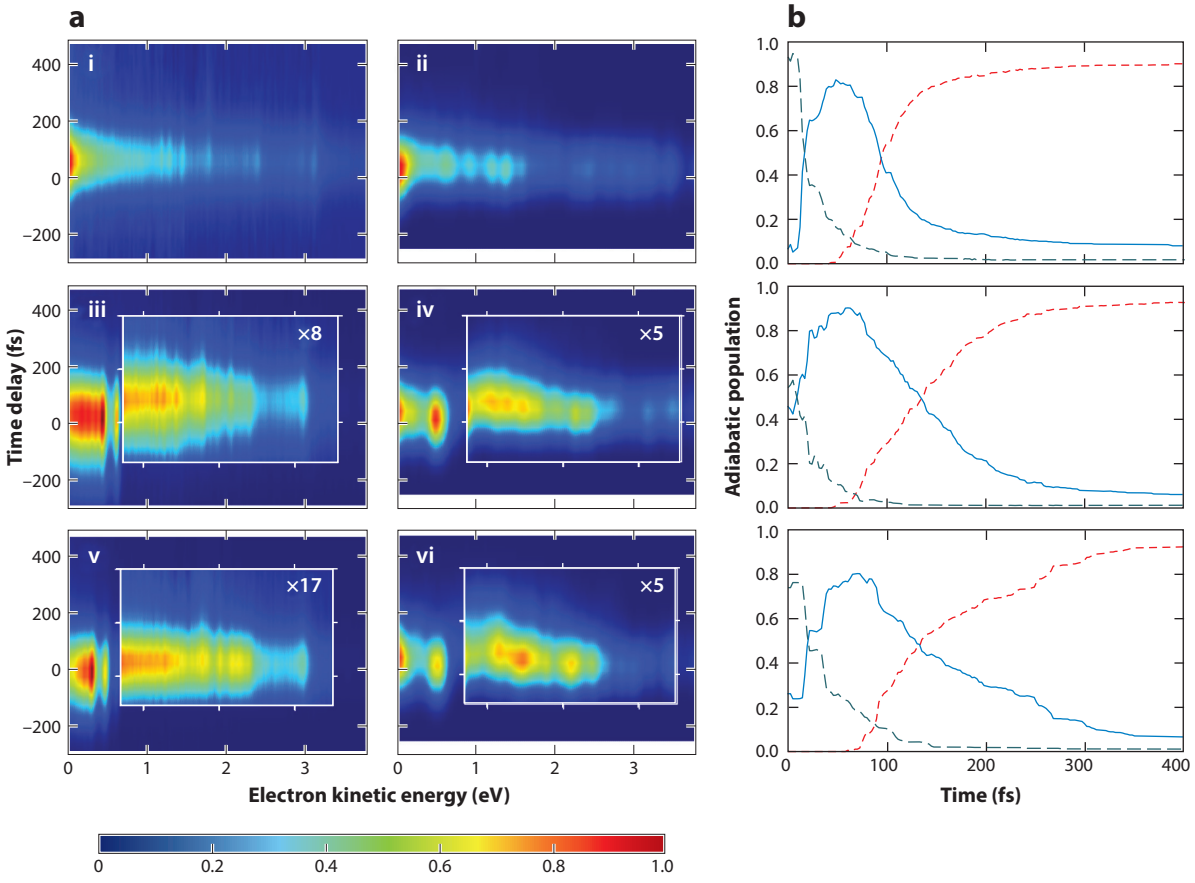

Figure 6

(*a*) Time-resolved photoelectron spectra of acrylonitrile (AN) (*i*,*ii*), 2-methacrylonitrile/*cis*-crotonitrile (CrN) (*iii*,*iv*), and *cis*-3-methylacrylonitrile (MeAN) (*v*,*vi*). Both experimental spectra (*i*,*iii*,*v*) and ab initio multiple spawning (AIMS) simulated spectra (*ii*,*iv*,*vi*) are shown. (*b*) The adiabatic state populations extracted from the AIMS simulations show an increasing excited-state lifetime on going from AN (*top*) to CrN (*middle*) to MeAN (*bottom*).

lifetime of MeAN would be roughly equivalent to that of AN (since pyramidalization would occur at the terminal C3 CH_2 group, which is still free to twist). In contrast, the excited-state lifetime of CrN would be expected to be significantly longer, since pyramidalization would necessarily occur at an inertially constrained site, namely either the cyano-substituted C2 or the methyl-substituted C3. Interestingly, precisely the opposite behavior was observed. The excited-state decay of the MeAN population, as evidenced by time constants fit to the TRPES spectra, was nearly twice as long (99 fs) as that measured for AN (53 fs), whereas that for CrN was intermediate between those of AN and MeAN (see **Figure 6**). These results were in excellent agreement with the ab initio simulations, which provided mechanistic insight into the observations. The prediction that the MeAN timescales should be similar to those of AN emerges from the naive assumption that it is the inertial effect of the methyl groups that determines excited decay rates. However, such an analysis fails to recognize that the cyano group has a significant effect on the relevant electronic states, that is, a potential effect.

Pyramidalization at an ethylenic carbon in a $\pi\pi^*$ state is accompanied by a sudden polarization across the carbon–carbon double bond (65). The cyano group, a π donor, strongly stabilizes the formation of a negative charge at the adjacent C2. Thus, as confirmed by the AIMS results, pyramidalization occurs almost exclusively at the C2, regardless of where the methyl group is located. Optimization of the corresponding minimum-energy CIs confirms that structures involving pyramidalization at the C2 are more than 1 eV lower in energy than structures in which pyramidalization occurs at the C3 (in ethylene the analogous structures are degenerate). In this way, the cyano substituent tilts the potential energy surfaces toward a particular CI by stabilizing the adjacent negative charge associated with these structures. Furthermore, these results hint at a possible chemical control strategy for directing excited nonadiabatic dynamics in polyenes via the site-specific stabilization of the charges associated with the large-amplitude twist-pyramidalization motions governing passage through CIs in these molecules. Supporting this perspective, we note that the effects of heteroatoms on photoisomerization (for the case of the hemithioindigo molecule) were previously discussed in terms of the electron-donating or electron-withdrawing character of the heteroatom (72). Furthermore, the role of transient charge stabilization in photoisomerization, more generally, has also been previously documented (73, 74). An important example of such potential effects in ultrafast dynamics at CIs is seen in the role of the protein environment on the bond selectivity of *cis-trans* isomerization in the retinal protonated Schiff base, shown to be a key factor in altering the local CI topography, thereby explaining the remarkable propensity for forming the 11-*cis* photoproduct (40). We anticipate that systematic studies, using selective chemical substitution, of potential effects due to heteroatoms on dynamics at CIs will lead to simple models and intuitive approaches to a more dynamical picture of branching and selectivity in excited-state photochemistry.

5. THE ROLE OF LARGE-AMPLITUDE VIBRATIONAL MOTION IN THE LOCALIZATION OF EXCITED-STATE DYNAMICS

5.1. The Dynamophore

Chemical substitution can also be employed to connect multiple chromophores or distinct chemical moieties. How these constituent components are connected can dramatically influence the resulting nonadiabatic dynamics. Since the C=C bond is the common chromophore in many systems, we might hope that the extensive work studying excited-state dynamics at an isolated C=C bond (ethylene) might form a basis for understanding the excited-state dynamics in the larger polyenes. To what extent is this the case? Again, we believe that a phenomenological approach is required, at least initially. Examples we have considered include linear [1,3-butadiene (75) and 2,4,6,8-decatetraene (76)] and cyclic [cyclopentadiene (77), 1,4-cyclohexadiene (CHD) (17), and cycloheptatriene (78)] polyenes.

As discussed in Section 1, it is convenient for this discussion to introduce the concept of a dynamophore (17), a direct analog to the idea of a chromophore. A chromophore is the part of a molecular entity in which the electronic transition responsible for a given spectral band is approximately localized (79). Both $\pi\pi^*$ and π3s transitions, for example, make use of the same chromophore: a π-orbital. Because the π-orbitals of small molecules are commonly delocalized over the whole conjugated or homoconjugated π-system, the excitation is therefore necessarily delocalized. By contrast, an $n\pi^*$-transition is often a localized excitation at, for example, a C=O or an N–H subunit. Analogous to the concept of a chromophore, a dynamophore is the part of the molecule where the dynamics are approximately localized. While the initial response is governed by Franck–Condon active modes, the nonadiabatic transitions between electronic states often arise

from a small subset of distinct molecular displacements which may, or may not, be localized on a specific part of the molecular frame. As discussed below, we find that thinking in terms of how dynamics localize, or not, around a molecular subunit is a useful and instructive perspective, as larger molecules often contain the same subunits (e.g., a C=C bond).

5.2. Cyclohexadiene: Absorb Globally, Act Locally

When molecules absorb UV light, the electronic transitions are between eigenstates distributed over the molecular frame. In other words, the excitation is delocalized. However, in many cases, the reaction dynamics are local, sometimes centered on a specific moiety or chemical bond. How and when does a delocalized excitation become dynamically localized? In order to address this question, we compared the dynamics of CHD, which exhibits the through-bond interaction of homoconjugation (electronic interaction between nonconjugated double bonds), with the singly C=C bonded cyclohexene (CHE) (17).

For reference, the energetic splitting between the in-phase and out-of-phase combinations of the two ethylenic C=C units in the homoconjugated CHD is about 1 eV, and about 2 eV in the π-conjugated 1,3-cyclohexadiene. This indicates that homoconjugation has a major effect on the electronic structure of CHD and leads to the intuition that its excited-state dynamics should remain delocalized, as is known to be the case for 1,3-cyclohexadiene (80). CHD and CHE were each excited (200-nm pump pulse) to their respective 3s Rydberg state, and their subsequent dynamics were studied by TRPES and by ab initio dynamics simulations. The prepared 3s Rydberg state decays via a CI with a lower-lying dark $\pi\pi^*$ state and finally to the ground state, thus forming a hot molecule as suggested by **Figure 7**.

Remarkably, the TRPES spectra of CHD and CHE reveal very similar subpicosecond time constants and decay-associated photoelectron spectra. Dynamically, the homoconjugated CHD seems to behave in the same way as CHE (with a single C=C bond), despite the fact that the initial excitation is delocalized over both ethylene subunits. To support this observation, our ab initio calculations show that CHD and CHE have geometrically similar, energetically accessible CIs. Overall, our results indicate that the excited-state dynamics of CHD become rapidly localized at a single C=C double bond and that the effects of strong through-bond interaction (homoconjugation), dominant in the absorption spectrum, are absent in the dynamics. What is the origin of this behavior?

For dynamics to localize, we require interactions that will couple the in-phase (V_+) and out-of-phase (V_-) electronic wave functions, leading to localization on only one C=C bond. In CHD, the through-bond coupling between the ethylenic units is mediated by the σ-orbitals forming the C–H bonds on the bridging C atoms, as illustrated in **Figure 7**. The through-bond interaction is strong at the Franck–Condon geometry, leading to large 1-eV splitting of the in-phase and out-of-phase $\pi\pi^*$ combinations. Because of the p-orbital-like structure of the C–H bonds, the through-bond coupling is highly sensitive to displacement or distortion of the bridging CH_2 units, indicated by the coordinate Q. These displacements, which involve both translation of the bridging CH_2 and angular deformation of the C–H bonds, rapidly reduce the electronic coupling and, hence, the associated energetic splitting between the in-phase and out-of-phase combinations, so that they approach degeneracy at large Q (distorted geometries), as illustrated in the energy level scheme in **Figure 7**. Near degeneracy, any other molecular vibration of the appropriate symmetry can nonadiabatically mix these two combinations, thereby leading to a localization of excitation on a single C=C bond. Once dynamical localization occurs, rapid ethylenic dynamics (i.e., twisting and pyramidalization) occur at a single C=C bond, leading to apparently irreversible decay to the ground state. Thus, homoconjugated CHD behaves dynamically as does the singly

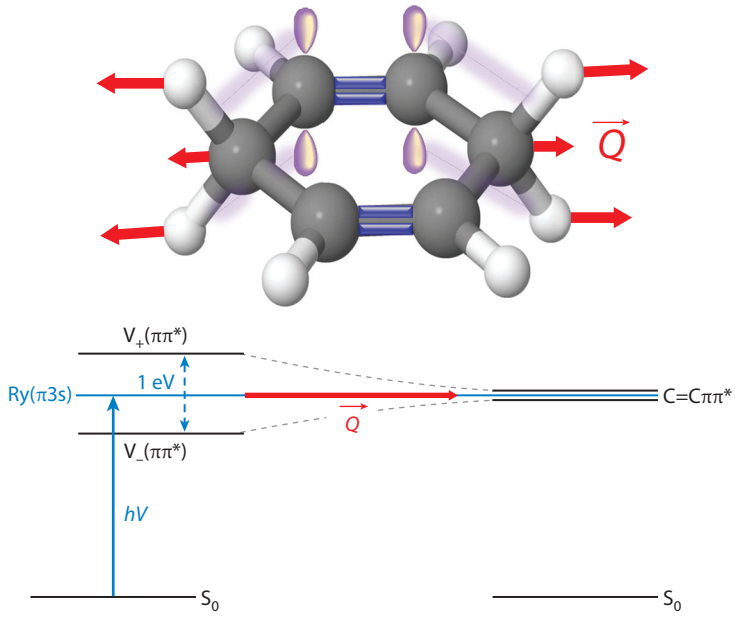

Figure 7

In 1,4-cyclohexadiene (CHD), through-bond coupling of the two C=C ethylene subunits (*blue*) is mediated by the p-orbitals on the bridging CH_2 units. The coupling is strong and leads to a 1-eV splitting in the UV absorption spectrum of the in-phase (V_+) and out-of-phase (V_-) $\pi\pi^*$ combinations (*bottom left*). This coupling, however, is very sensitive to distortions of the bridging CH_2 units. Specific large-amplitude motions, indicated by the coordinate Q, rapidly decouple the two ethylenic units, and they therefore approach degeneracy as a function of Q (*bottom right*). Near degeneracy, any other vibration of the correct symmetry will nonadiabatically mix (V_+) and (V_-), leading to localization on a single C=C bond. Once localization is achieved, the system behaves as would any alkyl substituted ethylene: It rapidly passes through a Tw-Py (twisting followed by pyramidalization) CI to the ground state. Remarkably, CHD behaves dynamically as does cyclohexene (with a single C=C bond), despite the fact that the initial excitation was delocalized over the entire molecular frame.

C=C bonded CHE. The dynamophore in CHD is the C=C bond. In contrast, the conjugated 1,3-cyclohexadiene can never distort enough in the excited state to break the coupling between its adjacent C=C bonds and, therefore, the dynamophore in 1,3-cyclohexadiene remains the same as its chromophore, the conjugated C=C–C=C subunit of the ring.

We speculate that there is great utility in understanding which vibrational motions may drive dynamical localization versus those which retain delocalized behavior. We suggest that the concept of a dynamophore serves to bring this idea into focus.

6. CONCLUSIONS AND OUTLOOK

We have shown how a strategy that employs functional group substitution and selective methylation of organic chromophores can be used to influence and therefore probe new details of ultrafast CI-mediated dynamics in excited states. Our standard method for interrogating these photoinitiated dynamics involves coordination of experimental and theoretical efforts in the form of TRPES and the simulation of the resultant spectra using ab initio dynamics simulations. On the basis of numerous such studies, we believe we are now in a position to place these many

phenomenological observations into a broader context. Organic chemists have, for over a century, used chemical substitutions to understand structure–function relationships. We argue that this same approach can be used to develop dynamics–function relationships. We have shown that standard methods in chemical synthesis have the capacity to probe dynamics at CIs in photochemical processes. As the underlying mechanistic details of the nonradiative decay pathways, both in terms of the electronic structure and nuclear dynamics, are more clearly elucidated, this may be accomplished in an increasingly prescriptive manner. The results described here collectively suggest two primary vectors of probing dynamics at CIs: (*a*) by influencing or directing the momentum of the excited-state wave packet along coordinates involving large-amplitude motion (a general characteristic of dynamics in unsaturated organic molecules) and (*b*) by employing functional group substitution to affect the seam of a CI via electronic structure. Specifically, the charge separation that develops across C=C bonds at common CI motifs in unsaturated molecules, together with the chemistry that can be employed to selectively stabilize these charges at particular atomic sites, is an example of such chemical control.

More generally, what has become clear is that microcanonical, transition-state theories that have been so successfully used to describe some ground-state chemical processes will fail to describe many excited-state processes, particularly those in which passage through regions of strong nonadiabatic coupling between electronic states is characterized by timescales on the order of a vibrational period. We argue that there is a need for a dynamical approach to these excited-state processes, perhaps drawing lessons from the well-known dynamics at transition states in ground-state reaction dynamics. We hope that our phenomenological studies will help inspire the development of new dynamical theories for nonadiabatic processes at CIs.

DISCLOSURE STATEMENT

The authors are not aware of any affiliations, memberships, funding, or financial holdings that might be perceived as affecting the objectivity of this review.

ACKNOWLEDGMENTS

We thank Todd J. Martínez for many helpful and encouraging discussions on dynamics at conical intersections. We thank our many coworkers, in particular A.E. Boguslavskiy, O. Schalk, S. Neville and R.J. MacDonell, for their contributions to this work. M.S.S. and A.S. each acknowledge funding from the National Science and Engineering Research Council of Canada through the Discovery grant program.

LITERATURE CITED

1. Michl J, Bonačić-Koutecký V. 1990. *Electronic Aspects of Organic Photochemistry*. New York: Wiley
2. Yarkony DR. 2004. Conical intersections: their description and consequences. In *Conical Intersections: Electronic Structure, Dynamics and Spectroscopy*, ed. W Domcke, DR Yarkony, H Köppel, pp. 41–128. Singapore: World Sci.
3. Worth GA, Cederbaum LS. 2004. Beyond Born–Oppenheimer: molecular dynamics through a conical intersection. *Annu. Rev. Phys. Chem.* 55:127–58
4. Levine B, Martínez T. 2007. Isomerization through conical intersections. *Annu. Rev. Phys. Chem.* 58:613–34
5. Matsika S, Krause P. 2011. Nonadiabatic events and conical intersections. *Annu. Rev. Phys. Chem.* 62:621–43

6. Richter M, Marquetand P, González-Vázquez J, Sola I, González L. 2011. SHARC: ab inito molecular dynamics with surface hopping in the adiabatic representation including arbitrary couplings. *J. Chem. Theor. Comput.* 7:1253–58
7. Ashfold M, Devine A, Dixon R, King G, Nix M, Oliver T. 2008. Exploring nuclear motion through conical intersections in the UV photodissociation of phenols and thiophenol. *PNAS* 105:12701–6
8. Marchetti B, Karsili T, Ashfold M, Domcke W. 2016. A 'bottom up', ab initio computational approach to understanding fundamental photophysical processes in nitrogen containing heterocycles, DNA bases and base pairs. *Phys. Chem. Chem. Phys.* 18:20007–27
9. Ashfold M, Bain M, Hansen C, Ingle R, Karsili T, et al. 2017. Exploring the dynamics of the photoinduced ring-opening of heterocyclic molecules. *J. Phys. Chem. Lett.* 8:3440–51
10. Klessinger M. 1995. Conical intersections and the mechanism of singlet photoreactions. *Angew. Chem. Int. Ed.* 34:549–51
11. Bernardi F, Olivucci M, Robb MA. 1996. Potential energy surface crossings in organic photochemistry. *Chem. Soc. Rev.* 25:321–28
12. Pechukas P. 1981. Transition-state theory. *Annu. Rev. Phys. Chem.* 32:159–77
13. Truhlar D, Garrett B, Klippenstein S. 1996. Current status of transition state theory. *J. Phys. Chem.* 100:12771–800
14. Miller W. 1998. Spiers memorial lecture: Quantum and semiclassical theory of chemical reaction rates. *Faraday Discuss.* 110:1–21
15. Guo H, Jiang B. 2014. The sudden vector projection model for reactivity: mode specificity and bond selectivity made simple. *Acc. Chem. Res.* 47:3679–85
16. Ma X, Hase W. 2017. Perspective: Chemical dynamics simulations of non-statistical reaction dynamics. *Phil. Trans. R. Soc. A* 375:20160204
17. Schalk O, Boguslavskiy A, Stolow A, Schuurman M. 2011. Through-bond interactions and the localization of excited state dynamics. *J. Am. Chem. Soc.* 133:16451–58
18. Malhado J, Hynes J. 2016. Non-adiabatic transition probability dependence on conical intersection topography. *J. Chem. Phys.* 145:194104
19. Stolow A. 2003. Femtosecond time-resolved photoelectron spectroscopy of polyatomic molecules. *Annu. Rev. Phys. Chem.* 54:89–119
20. Stolow A, Bragg A, Neumark D. 2004. Femtosecond time-resolved photoelectron spectroscopy. *Chem. Rev.* 104:1719–57
21. Suzuki T. 2006. Femtosecond time-resolved photoelectron imaging. *Annu. Rev. Phys. Chem.* 57:555–92
22. Stolow A, Underwood J. 2008. Time-resolved photoelectron spectroscopy of nonadiabatic dynamics in polyatomic molecules. *Adv. Chem. Phys.* 139:497–583
23. Stock G, Domcke W. 1997. Theory of ultrafast nonadiabatic excited-state processes and their spectroscopic detection in real time. *Adv. Chem. Phys.* 100:1–169
24. Seideman T. 2002. Time-resolved photoelectron angular distributions: concepts, applications, and directions. *Annu. Rev. Phys. Chem.* 53:41–65
25. Reid KL. 2003. Photoelectron angular distributions. *Annu. Rev. Phys. Chem.* 54:397–424
26. Wang K, McKoy V, Hockett P, Schuurman MS. 2014. Time-resolved photoelectron spectra of CS_2: dynamics at conical intersections. *Phys. Rev. Lett.* 112:113007
27. Martínez TJ, Ben-Nun M, Levine RD. 1996. Multi-electronic-state molecular dynamics: a wave function approach with applications. *J. Phys. Chem.* 100:7884–95
28. Martínez TJ, Ben-Nun M, Levine RD. 1997. Molecular collision dynamics on several electronic states. *J. Phys. Chem. A* 101:6389–402
29. Ben-Nun M, Quenneville J, Martínez TJ. 2000. Ab initio multiple spawning: photochemistry from first principles quantum molecular dynamics. *J. Phys. Chem. A* 104:5161–75
30. Ben-Nun M, Martínez TJ. 1998. Nonadiabatic molecular dynamics: validation of the multiple spawning method for a multidimensional problem. *J. Chem. Phys.* 108:7244–57
31. Ben-Nun M, Martínez TJ. 2002. Ab initio quantum molecular dynamics. *Adv. Chem. Phys.* 121:439–512
32. Virshup AM, Punwong C, Pogorelov TV, Lindquist BA, Ko C, Martínez TJ. 2009. Photodynamics in complex environments: ab initio multiple spawning quantum mechanical/molecular mechanical dynamics. *J. Phys. Chem. B* 113:3280–91

33. Tully JC, Preston RK. 1971. Trajectory surface hopping approach to nonadiabatic molecular collisions: the reaction of H^+ with D_2. *J. Chem. Phys.* 55:562–72
34. Tully JC. 1990. Molecular dynamics with electronic transitions. *J. Chem. Phys.* 93:1061–71
35. Worth GA, Burghardt I. 2003. Full quantum mechanical molecular dynamics using Gaussian wavepackets. *Chem. Phys. Lett.* 368:502–8
36. Richings G, Polyak I, Spinlove K, Worth G, Burghardt I, Lasorne B. 2015. Quantum dynamics simulations using Gaussian wavepackets: the vMCG method. *Int. Rev. Phys. Chem.* 34:269–308
37. Saita K, Shalashilin DV. 2012. On-the-fly ab initio molecular dynamics with multiconfigurational Ehrenfest method. *J. Chem. Phys.* 137:22A506
38. Atchity Y, Xantheas X, Rudenberg K. 1991. Potential energy surfaces near intersections. *J. Chem. Phys.* 95:1862–76
39. Yarkony DR. 2001. Nuclear dynamics near conical intersections in the adiabatic representation: I. The effects of local topography on interstate transitions. *J. Chem. Phys.* 114:2601–13
40. Ben-Nun M, Molnar F, Schulten K, Martínez TJ. 2002. The role of intersection topography in bond selectivity of *cis-trans* photoisomerization. *PNAS* 99:1769–73
41. Silicia F, Blancafort L, Bearpark M, Robb M. 2007. Quadratic description of conical intersections: characterization of critical points on the extended seam. *J. Phys. Chem. A.* 11:2182–92
42. Krause P, Matsika S, Kotur M, Weinacht T. 2002. The influence of excited state topology on wavepacket delocalization in the relaxation of photoexcited polyatomic molecules. *J. Chem. Phys.* 137:22A537
43. Yarkony DR. 2005. Statistical and nonstatistical nonadiabatic photodissociation from the first excited state of the hydroxymethyl radical. *J. Chem. Phys.* 122:084316
44. Freed KF. 1976. Energy dependence of electronic relaxation processes in polyatomic molecules. In *Radiationless Processes in Molecules and Condensed Phases*, ed. FK Fong, pp. 23–168. Berlin: Springer
45. Avouris P, Gelbart WM, El-Sayed MA. 1977. Nonradiative electronic relaxation under collision-free conditions. *Chem. Rev.* 77:793–833
46. Penner AP, Siebrand W, Zgierski MZ. 1978. Radiationless decay of vibronically coupled electronic states. *J. Chem. Phys.* 69:5496–508
47. Köppel H, Domcke W, Cederbaum LS. 1984. Multimode molecular dynamics beyond the Born–Oppenheimer approximation. *Adv. Chem. Phys.* 57:59–246
48. Köppel H, Domcke W, Cederbaum LS. 2004. The multi-mode vibronic-coupling approach. In *Conical Intersections: Electronic Structure, Dynamics and Spectroscopy*, ed. W Domcke, DR Yarkony, H Köppel, pp. 323–68. Singapore: World Sci.
49. Hazra A, Nooijen M. 2005. Comparison of various Franck–Condon and vibronic coupling approaches for simulating electronic spectra: the case of the lowest photoelectron band of ethylene. *Phys. Chem. Chem. Phys.* 7:1759–71
50. Klein K, Garand E, Ichino T, Neumark DM, Gauss J, Stanton JF. 2011. Quantitative vibronic coupling calculations: the formyloxyl radical. *Theor. Chem. Acc.* 129:527–43
51. Dillon J, Yarkony DR, Schuurman MS. 2011. On the construction of quasidiabatic state representations of bound adiabatic state potential energy surfaces coupled by accidental conical intersections: incorporation of higher order terms. *J. Chem. Phys.* 134:044101
52. Rabidoux SM, Eijkhout V, Stanton JF. 2014. Parallelization strategy for large-scale vibronic coupling calculations. *J. Phys. Chem. A* 118:12059–68
53. Fuß W. 2013. Where does the energy go in fs-relaxation? *Chem. Phys.* 425:96–103
54. Fuß W. 2015. Predistortion amplified in the excited state. *J. Photochem. Photobiol. A* 297:45–57
55. Barbatti M, Paier J, Lischka H. 2004. Photochemistry of ethylene: a multireference configuration interaction investigation of the excited-state energy surfaces. *J. Chem. Phys.* 121:11614–24
56. Tao H, Allison TK, Wright TW, Stooke AM, Khurmi C, et al. 2011. Ultrafast internal conversion in ethylene. I. The excited state lifetime. *J. Chem. Phys.* 134:244306
57. Allison TK, Tao H, Glover WJ, Wright TW, Stooke AM, et al. 2012. Ultrafast internal conversion in ethylene. II. Mechanisms and pathways for quenching and hydrogen elimination. *J. Chem. Phys.* 136:124317
58. Mori T, Glover WJ, Schuurman MS, Martínez TJ. 2012. Role of Rydberg states in the photochemical dynamics of ethylene. *J. Phys. Chem. A* 116:2808–18

59. Kobayashi T, Horio T, Suzuki T. 2015. Ultrafast deactivation of the $\pi\pi^*(V)$ state of ethylene studied using sub-20 fs time-resolved photoelectron imaging. *J. Phys. Chem. A* 119:9518–23
60. Champenois EG, Shivaram NH, Wright TW, Yang CS, Belkacem A, Cryan JP. 2016. Involvement of a low-lying Rydberg state in the ultrafast relaxation dynamics of ethylene. *J. Chem. Phys.* 144:014303
61. Ben-Nun M, Martínez TJ. 2000. Photodynamics of ethylene: ab initio studies of conical intersections. *Chem. Phys.* 259:237–48
62. Quenneville J, Ben-Nun M, Martínez TJ. 2001. Photochemistry from first principles advances and future prospects. *J. Photochem. Photobiol. A: Chem.* 144:229–35
63. Barbatti M, Ruckenbauer M, Lischka H. 2005. The photodynamics of ethylene: a surface-hopping study on structural aspects. *J. Chem. Phys.* 122:174307
64. Tao H, Levine BG, Martínez TJ. 2009. Ab initio multiple spawning dynamics using multi-state second-order perturbation theory. *J. Phys. Chem. A* 113:13656–62
65. Brooks BR, Schaefer HF. 1979. Sudden polarization: pyramidalization of twisted ethylene. *J. Am. Chem. Soc.* 101:307–11
66. Bonačić-Koutecký V, Bruckmann P, Hiberty P, Koutecký J, Leforestier C, Salem L. 1975. Sudden polarization in the zwitterionic Z_1 excited states of organic intermediates. Photochemical implications. *Angew. Chem. Int. Ed.* 14:575–76
67. Wu G, Boguslavskiy AE, Schalk O, Schuurman M, Stolow A. 2011. Ultrafast non-adiabatic dynamics of methyl substituted ethylenes: the $\pi 3s$ Rydberg state. *J. Chem. Phys.* 135:164309
68. Lee A, Coe J, Ho M, Lee S, Cheng B, et al. 2007. Substituent effects on dynamics at conical intersections: α,β-enones. *J. Phys. Chem.* 111:11948–60
69. Neville S, Wang Y, Boguslavskiy A, Stolow A, Schuurman M. 2016. Substituent effects on dynamics at conical intersections: allene and methyl allenes. *J. Chem. Phys.* 144:014305
70. Hudock HR, Levine BG, Thompson AL, Satzger H, Townsend D, et al. 2007. Ab initio molecular dynamics and time-resolved photoelectron spectroscopy of electronically excited uracil and thymine. *J. Phys. Chem. A* 111:8500–8
71. MacDonell RJ, Schalk O, Geng T, Thomas RD, Feifel R, et al. 2016. Excited state dynamics of acrylonitrile: substituent effects at conical intersections interrogated via time-resolved photoelectron spectroscopy and ab initio simulation. *J. Chem. Phys.* 145:114306
72. Nenov A, Cordes T, Herzog T, Zinth W, de Vivie-Riedle R. 2010. Molecular driving forces for Z/E isomerization mediated by heteroatoms: the example hemithioindigo. *J. Phys. Chem. A.* 114:13016–30
73. Martínez TJ. 2006. Insights for light-driven molecular devices from ab initio multiple spawning excited-state dynamics of organic and biological chromophores. *Acc. Chem. Res.* 39:119–26
74. Virshup AM, Levine BG, Martínez TJ. 2014. Steric and electrostatic effects on photoisomerization dynamics using QM/MM ab initio multiple spawning. *Theor. Chem. Acc.* 133:1506
75. Hockett P, Ripani E, Rytwinski A, Stolow A. 2013. Probing ultrafast dynamics with time-resolved multi-dimensional coincidence imaging: butadiene. *J. Mod. Opt.* 60:1409–25
76. Blanchet V, Zgierski MZ, Seideman T, Stolow A. 1999. Discerning vibronic molecular dynamics using time-resolved photoelectron spectroscopy. *Nature* 401:52–54
77. Schalk O, Boguslavskiy A, Stolow A. 2010. Substituent effects on dynamics at conical intersections: cyclopentadienes. *J. Phys. Chem. A* 114:4058–64
78. Schalk O, Boguslavskiy A, Schuurman M, Brogaard R, Unterreiner A, et al. 2013. Substituent effects on dynamics at conical intersections: cycloheptatrienes. *J. Phys. Chem. A* 117:10239–47
79. McNaught AD, Wilkinson A. 1997. *IUPAC Compendium of Chemical Terminology*. Oxford: Blackwell Sci. 2nd ed.
80. Deb S, Weber P. 2011. The ultrafast pathway of photon-induced electrocyclic ring-opening reactions: the case of 1,3-cyclohexadiene. *Annu. Rev. Phys. Chem.* 62:19–39

Annual Review of
Physical Chemistry
Volume 69, 2018

Contents

Indexes

Errata

An online log of corrections to *Annual Review of Physical Chemistry* articles may be found at http://www.annualreviews.org/errata/physchem